JOURNAL OF MAGNETIC RESONANCE **126,** 266–269 (1997)
ARTICLE NO. MN971171

NOTES

Effect of Long TE on T_1 Measurement in STEAM Progressive Saturation Experiment

Jack Knight-Scott* and Shi-Jiang Li

Biophysics Research Institute, Medical College of Wisconsin, 8701 Watertown Plank Road, Milwaukee, Wisconsin 53226

Received August 19, 1996; revised March 26, 1997

Progressive saturation (*1*) is the most widely used longitudinal relaxation measurement technique in localized clinical proton magnetic resonance spectroscopy. When flip angles and frequency settings are near ideal, peak signal intensities from a single-pulse progressive saturation (PS) experiment can be shown to obey (*1*)

$$S(\mathrm{TD}) = S_0[1 - \exp(-\mathrm{TD}/T_1)], \qquad [1]$$

where $S(\mathrm{TD})$ is the signal intensity as a function of the delay time (TD), T_1 is the longitudinal relaxation time, and S_0 is the signal intensity when $\mathrm{TD} \gg T_1$. For the original single-pulse PS sequence, TD is equal to the repetition time (TR), and Eq. [1] may be rewritten as

$$S(\mathrm{TR}) = S_0[1 - \exp(-\mathrm{TR}/T_1)]. \qquad [2]$$

Recent ^{1}H MRS studies have measured the T_1 of metabolites using long echo times in the spectroscopic stimulated echo acquisition mode (STEAM) localization sequence (*2–7*), and fitted to Eq. [2].

Unfortunately, for multipulse sequences, Eq. [2] no longer accurately describes the longitudinal relaxation behavior, even if ideal conditions of perfect RF pulses and negligible off-resonance effects are assumed. For STEAM at short echoes times (TE) and short mixing times (TM), relative to T_1, Eq. [2] is a valid approximation, but it begins to fail as TE and/or TM increases, giving elevated T_1 values for increasing TE and/or TM. Although Eq. [1] has been previously employed as a correction factor for localized STEAM ^{1}H MRS concentration measurements (*8, 9*), to our knowledge, specific derivation of the equation and examination of PS dependence on TE or TM has not been investigated. This Note presents an analytical derivation of the equation, using an approach similar to that of Shoup, Becker, and Farrar (*10*), for a STEAM sequence to evaluate the effects of TE on the T_1 measurement of the progressive saturation experiment. Results from simulations and measurements performed on a phantom are also presented.

For simplicity, we will exclude coupling effects, and assume off-resonance and diffusion effects are negligible, all flip angles are perfect 90°, spin–spin relaxation (T_2') dominates the natural transverse relaxation (T_2), i.e., $T_2 \approx T_2'$, *and* B_0 inhomogeneity is dominated by the application of crusher gradients. The influence of slice-selective gradients can be ignored if the gradients are balanced with rephasers to correct for dephasing caused by the application of these gradient pulses. Since we are interested in relaxation effects, it is easier to follow the macroscopic magnetization, i.e., the ''ensemble average,'' at particular points in time than to analyze the effects of the sequence on individual spin systems where we must be concerned with coupling effects.

Let M_0 represent the macroscopic thermal equilibrium magnetization, and M_z and M_{xy} the net macroscopic longitudinal and transverse magnetization in the rotating frame, respectively, for a group of equivalent spins with $I = \frac{1}{2}$. For the STEAM sequence shown in Fig. 1, all pulses are $90°_{-x}$. Immediately following the first pulse at time $t = 0_+$, the longitudinal magnetization is rotated into the transverse plane such that the longitudinal (z) and transverse (xy) components are given by

$$M_z(0_+) = 0 \qquad [3]$$

$$M_{xy}(0_+) = M_z(0_-).$$

We assume that the net transverse magnetization immediately before the first pulse is equal to zero. This condition may be easily met by allowing at least $3T_2^*$ for acquisition, or applying a homospoil gradient pulse at the end of the sequence.

Over the interval τ_1–0, the longitudinal magnetization recovers toward M_0, while the xy component decays at a natural rate of $1/T_2$. The transverse magnetization is also dephased by application of crusher gradient $\mathbf{G}_1$, such that immediately before the second pulse at $t = \tau_1$,

$$M_z(\tau_{1-}) = M_0[1 - \exp(-\tau_1/T_1)]$$

$$M_{xy}(\tau_{1-}) = M_z(0_-)\exp(-\tau_1/T_2) \times \overline{\exp(-i\gamma\int\int \mathbf{G}_1 \cdot d\mathbf{r}\, dt)} = 0. \qquad [4]$$

* Currently at the Health Sciences Center, Department of Radiology, University of Virginia, Box 170, Charlottesville, Virginia 22908.

1090-7807/97 $25.00

The ensemble average of the *xy* component is equal to zero for large values of $\int \mathbf{G}_1(t)dt$. However, we will follow $M_{xy}(\tau_{1-})$ since it will later lead to the stimulated echo (*11*). Immediately after the second pulse part of $M_{xy}(\tau_{1-})$ is stored along the longitudinal axis, while the net transverse magnetization is now composed of the previously recovered longitudinal magnetization and the remaining part of $M_{xy}(\tau_{1-})$:

$$\begin{aligned} M_z(\tau_{1+}) &= -M_z(0_-)\exp(-\tau_1/T_2) \\ &\quad \times \overline{\sin(\gamma\int\int \mathbf{G}_1 \cdot d\mathbf{r}\,dt)} = 0 \\ M_{xy}(\tau_{1+}) &= M_z(\tau_{1-}) + M_z(0_-) \\ &\quad \times \exp(-\tau_1/T_2)\overline{\cos(\gamma\int\int \mathbf{G}_1 \cdot d\mathbf{r}\,dt)}. \end{aligned} \quad [5]$$

Over the interval $\tau_2 - \tau_1$, the recovery of the longitudinal magnetization toward M_0 entails T_1 relaxation of the dephased $M_z(\tau_{1+})$, while the transverse magnetization undergoes T_2 relaxation as well as dephasing by $\mathbf{G}_2$:

$$\begin{aligned} M_z(\tau_{2-}) &= M_0[1 - \exp(-(\tau_2 - \tau_1)/T_1)] + M_z(\tau_{1+})\exp[-(\tau_2 - \tau_1)/T_1] \\ M_{xy}(\tau_{2-}) &= M_z(\tau_{1-})\exp[-(\tau_2 - \tau_1)/T_2]\overline{\exp(-i\gamma\int\int \mathbf{G}_2 \cdot d\mathbf{r}\,dt)} \\ &\quad + M_z(0_-)\exp(-\tau_2/T_2)\overline{\cos(\gamma\int\int \mathbf{G}_1 \cdot d\mathbf{r}\,dt)\exp(-i\gamma\int\int \mathbf{G}_2 \cdot d\mathbf{r}\,dt)} = 0. \end{aligned} \quad [6]$$

The final pulse creates a multitude of possible coherences in the transverse plane

$$\begin{aligned} M_z(\tau_{2+}) &= -M_z(\tau_{1-})\exp[-(\tau_2 - \tau_1)/T_2]\overline{\sin(\gamma\int\int \mathbf{G}_2 \cdot d\mathbf{r}\,dt)} \\ &\quad - M_z(0_-)\exp(-\tau_2/T_2)\overline{\cos(\gamma\int\int \mathbf{G}_1 \cdot d\mathbf{r}\,dt)\sin(\gamma\int\int \mathbf{G}_2 \cdot d\mathbf{r}\,dt)} = 0 \\ M_{xy}(\tau_{2+}) &= M_0\{1 - \exp[-(\tau_2 - \tau_1)/T_1]\} \\ &\quad - M_z(0_-)\exp(-\tau_1/T_2)\exp[-(\tau_2 - \tau_1)/T_1]\overline{i\,\sin(\gamma\int\int \mathbf{G}_1 \cdot d\mathbf{r}\,dt)} \\ &\quad + M_z(\tau_{1-})\exp[-(\tau_2 - \tau_1)/T_2]\overline{\cos(\gamma\int\int \mathbf{G}_2 \cdot d\mathbf{r}\,dt)} \\ &\quad + M_z(0_-)\exp(-\tau_2/T_2)\overline{\cos(\gamma\int\int \mathbf{G}_1 \cdot d\mathbf{r}\,dt)\cos(\gamma\int\int \mathbf{G}_2 \cdot d\mathbf{r}\,dt)}. \end{aligned} \quad [7]$$

At time τ_3, when the signal is acquired, the transverse magnetization has experienced gradient $\mathbf{G}_1$ and undergone T_2 relaxation

$$\begin{aligned} M_{xy}(\tau_3) &= M_0\{1 - \exp[-(\tau_2 - \tau_1)/T_1]\}\exp[-(\tau_3 - \tau_2)/T_2]\overline{\exp(-i\gamma\int\int \mathbf{G}_1 \cdot d\mathbf{r}\,dt)} \\ &\quad - M_z(0_-)\exp[-(\tau_2 - \tau_1)/T_1]\exp[-(\tau_3 - \tau_2 + \tau_1)/T_2]\,\overline{i\,\sin(\gamma\int\int \mathbf{G}_1 \cdot d\mathbf{r}\,dt)\exp(-i\gamma\int\int \mathbf{G}_1 \cdot d\mathbf{r}\,dt)} \\ &\quad + M_z(\tau_{1-})\exp[-(\tau_3 - \tau_1)/T_2]\overline{\cos(\gamma\int\int \mathbf{G}_2 \cdot d\mathbf{r}\,dt)\exp(-i\gamma\int\int \mathbf{G}_1 \cdot d\mathbf{r}\,dt)} \\ &\quad + M_z(0_-)\exp(-\tau_3/T_2)\overline{\cos(\gamma\int\int \mathbf{G}_1 \cdot d\mathbf{r}\,dt)\cos(\gamma\int\int \mathbf{G}_2 \cdot d\mathbf{r}\,dt)\exp(-i\gamma\int\int \mathbf{G}_1 \cdot d\mathbf{r}\,dt)}, \end{aligned} \quad [8]$$

such that the only nonzero element is the second term, our stimulated echo:

$$\begin{aligned} M_{xy}(\tau_3) &= -\tfrac{1}{2}M_z(0_-)\exp[-(\tau_3 + \tau_1 - \tau_2)/T_2] \\ &\quad \times \exp[-(\tau_2 - \tau_1)/T_1]. \end{aligned} \quad [9]$$

The longitudinal magnetization recovers until the sequence is repeated at time τ_4:

$$\begin{aligned} M_z(\tau_4) &= M_0\{1 - \exp[-(\tau_4 - \tau_2)/T_1]\} \\ &\quad + M_z(\tau_{2+})\exp[-(\tau_4 - \tau_2)/T_1]. \end{aligned} \quad [10]$$

Using the steady-state constraint that $M_z(\tau_4) = M_z(0_-)$, and ignoring contributions from the second term in $M_z(\tau_4)$ since its net signal is zero, we find that the steady-state transverse magnetization is

$$\begin{aligned} M_{xy}(\tau_3) &= -\tfrac{1}{2}M_0\{1 - \exp[-(\tau_4 - \tau_2)/T_1]\} \\ &\quad \times \exp[-(\tau_3 + \tau_1 - \tau_2)/T_2] \\ &\quad \times \exp[-(\tau_2 - \tau_1)/T_1]. \end{aligned} \quad [11]$$

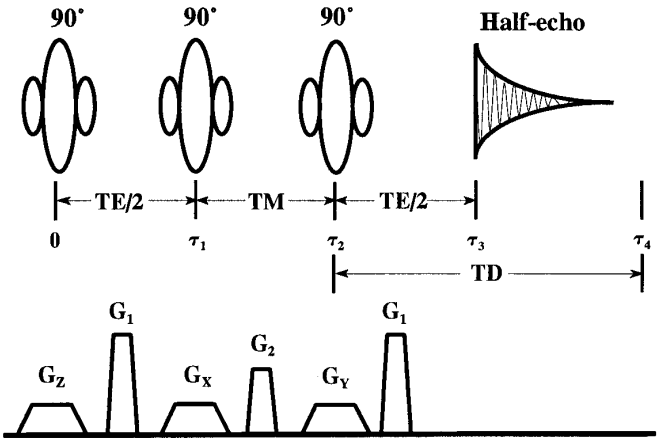

FIG. 1. Spectroscopic STEAM localization sequence. G_z, G_x, and G_y are slice-selective gradients applied along their respective axis. $\mathbf{G}_1$ and $\mathbf{G}_2$ are crushers of identical pulse lengths applied along all three axes. The τ values are the instantaneous times, whereas the echo time (TE), mixing time (TM), and delay time (TD) represent time intervals.

By replacing time differences with TR, TM, and TE, we now see how the steady-state magnetization varies as a function of TR:

$$M_{xy}(\mathrm{TR}) = M_{0_{\mathrm{TE,TM}}}\{1 - \exp[(\mathrm{TE}/2 + \mathrm{TM} - \mathrm{TR})/T_1]\}, \quad [12]$$

where

$$M_{0_{\mathrm{TE,TM}}} = -\tfrac{1}{2}M_0 \exp(-\mathrm{TM}/T_1 - \mathrm{TE}/T_2). \quad [13]$$

Equation [12] may be rewritten as

$$M_{xy}(\mathrm{TR}) = M_{0_{\mathrm{TE,TM}}}[1 - \exp(-\mathrm{TR}/\beta T_1)], \quad [14]$$

where

$$1/\beta = 1 - (\mathrm{TE}/2 + \mathrm{TM})/\mathrm{TR}. \quad [15]$$

Recognizing $\tau 4 - \tau 2$ in Eq. [11] as the delay time, the steady-state transverse magnetization as a function of TD may be written as

$$M_{xy}(\mathrm{TD}) = M_{0_{\mathrm{TE,TM}}}[1 - \exp(-\mathrm{TD}/T_1)]. \quad [16]$$

For non-zero TE and/or TM, β will always be greater than one, so the measured or apparent relaxation value (T_1^*), will be a weighted average of the various βT_1 values

$$T_1^* = \frac{\sum_{i=1}^{N} \alpha_i \beta_i T_1}{N}, \quad [17]$$

where N is the number of measurements used to describe the relaxation curve, and α values are weighting factors. Because α and β are functions of TR, TE, and TM, PS T_1 experiments that differ in any of these three parameters may yield different T_1^* values. The correction given in Eq. [12] removes these factors from the T_1 measurement.

A comparison of the differences obtained when using Eqs. [2] and [12] as models for T_1 data from a PS experiment is shown in Table 1 for a 500 ml distilled water sample containing 0.05 ml of Magnavist (Berlex Laboratories Inc., Wayne, New Jersey), a clinical contrast agent containing gadopentate dimeglumine. All measurements were performed on 1.5 T Magnetom Vision MRI whole-body system (Siemens Medical Systems, Erlanger, Germany) using a 27 cm diameter quadrature birdcage coil. A 2.5 × 2.5 × 2.5 cm volume was localized in the center of the phantom using a spectroscopic STEAM sequence. The latter half of the stimulated echo was acquired at TM = 10 ms, and TR = 12, 10, 7.5, 5, 4, 3, 2, 1.5, and 1.25 s for TE = 27, 60, 90, 135, and 270 ms. Stimulated echo data were apodized using a Gaussian filter (3 Hz line broadening), and zero-filled to 4K prior to FFT. Peak heights of the water resonance from magnitude spectra were used for all T_1 measurements to avoid possible phase errors. An iterative Marquardt–Levenberg algorithm provided in Sigma Plot (Jandel Corporation, San Rafael, California) was used to fit peak heights to Eqs. [2] and [12].

Accounting for the effects of partial saturation through the use of Eq. [12] reduces the error difference between the minimum and maximum T_1 values from 6 to 1%, while the coefficient of variance (CV) is reduced fourfold, 2.5% to less than 0.6%. This is in good agreement with simulations we performed. Assuming a T_1 of 2.0 s, a PS data set was simulated using Eq. [12] for TR = 10.0, 8.0, 7.0, 6.0, 5.0, 4.0, 3.0, 2.0, 1.5, and 1.25 s for TE = 30, 60, 90, 135, and 270 ms, and TM = 10 ms. The percent error between the minimum and maximum T_1 was 8%, and the CV was 3% when the simulated data was fitted to Eq. [2]. The scale of these errors may seem insignificant in comparison to the

TABLE 1
Correction of T_1 in the STEAM PS Experiment for TE-Dependent Partial Saturation Effects

	T_1 (s)	
TE (ms)	TD = TR	TD = TR − TE/2 − TM
27	2.274	2.215
60	2.297	2.215
90	2.298	2.197
135	2.326	2.193
270	2.432	2.190
Mean ± std. dev.	2.324 ± 0.059	2.202 ± 0.012
(CV)	(2.5%)	(0.5%)

large variance (20–50%) generally associated with spectroscopic T_1 measurements *in vivo* (*12*), but an assessment of these effects *in vivo* has yet to be made. The difference between short TE–TM and long TE–TM T_1 measurements will likely seem greater for measurements *in vivo* since macromolecular contributions from short T_1 species (*13*) at short TE–TM will result in a lower T_1 that is a weighted average of the relaxation times of the macromolecules and free metabolites. Given the variety of TEs and TRs used in localized STEAM experiments *in vivo*, correction of these errors may be essential for researchers who wish to compare results, especially in studies of T_1 as a possible indicator of pathology. Absolute quantitation methods that use internal water as a standard (*14*) may be particularly sensitive to changes in T_1, since the multicomponent nature of water in human brain (*15*) may account for substantial variations in T_1 with TE if left uncorrected.

Our analysis demonstrates that PS T_1 measurements using multipulse localization sequences such as STEAM are not only dependent on TR, but also on sequence parameters such as TE and TM. Any sequence that deviates from the single RF pulse and acquire technique must consider the effects of the additional RF pulses in the PS experiment. Although not shown here, a similar analysis may be performed for the point-resolved spectroscopy (PRESS) sequence (*16*).

ACKNOWLEDGMENTS

We thank Kathleen Donahue for her helpful comments. This work was supported by a grant from the National Cancer Institute, CA54600.

REFERENCES

1. R. Freeman and H. D. W. Hill, *J. Chem. Phys.* **54,** 3367–3377 (1971).
2. D. J. Manton, M. Lowry, S. J. Blackband, and A. Horsman, *NMR Biomed.* **8,** 104–112 (1995).
3. I. D. Wilkinson, M. Paley, W. K. Chong, B. J. Sweeney, J. K. Shepherd, B. E. Kendall, M. A. Hall-Craggs, and M. J. G. Harrison, *Magn. Reson. Imaging* **12,** 951–957 (1994).
4. K. Kamada, K. Houkin, K. Hida, H. Matsuzawa, Y. Iwasaki, H. Abe, and T. Nakada, *Magn. Reson. Med.* **31,** 537–540 (1994).
5. J. Granot, *J. Magn. Reson.* **70,** 488–492 (1986).
6. R. Kimmich and D. Hoepfel, *J. Magn. Reson.* **72,** 379–384 (1987).
7. J. Frahm, K.-D. Merboldt, and W. Hänicke, *J. Magn. Reson.* **72,** 502–508 (1987).
8. P. B. Barker, B. J. Soher, S. J. Blackband, J. C. Chatham, V. P. Mathews, and R. N. Bryan, *NMR Biomed.* **6,** 89–94 (1993).
9. R. Kreis, T. Ernst, and B. D. Ross, *Magn. Reson. Med.* **30,** 424–437 (1993).
10. R. R. Shoup, E. D. Becker, and T. C. Farrar, *J. Magn. Reson.* **8,** 298–310 (1972).
11. E. L. Hahn, *Phys. Rev.* **80,** 580–594 (1950).
12. O. Henriksen, *NMR Biomed.* **8,** 139–148 (1995).
13. K. L. Behar, D. L. Rothman, D. D. Spencer, and O. A. C. Petroff, *Magn. Reson. Med.* **32,** 294–302 (1994).
14. P. Christiansen, O. Henriksen, M. Stubgaard, P. Gideon, and H. B. W. Larsson, *Magn. Reson. Imaging* **11,** 107–118 (1993).
15. T. Ernst, R. Kreis, and B. D. Ross, *J. Magn. Reson. B* **102,** 1–8 (1993).
16. P. A. Bottomley, *Ann. N.Y. Acad. Sci.* **508,** 333–348 (1986).